Journal of Alloys and Compounds 408–412 (2006) 371–374

Journal of ALLOYS AND COMPOUNDS

www.elsevier.com/locate/jallcom

# $^{166}$Er and $^{155}$Gd Mössbauer spectroscopy of R–Rh–B (R = Er, Gd) system☆

Masuo Takeda[a,*], Junhu Wang[a], Masashi Takahashi[a], Toetsu Shishido[b], Akira Yoshikawa[b], Akio Nakamura[c]

[a] Department of Chemistry, Faculty of Science, Toho University, Funabashi, Chiba 274-8510, Japan
[b] Institute for Materials Research, Tohoku University, Katahira, Aoba-ku, Sendai 980-8577, Japan
[c] Advanced Science Research Center, Japan Atomic Energy Research Institute, Tokai, Ibaraki 319-1195, Japan

## Abstract

The eight compounds of R–Rh–B (R = Er, Gd) system have been studied by $^{166}$Er and $^{155}$Gd Mössbauer spectroscopy and DC magnetization measurements. Mössbauer spectroscopy revealed the bonding properties, charge distribution around the nucleus of the rare earth elements and the magnetic properties. Magnetic study has been done first for $ErRh_2$ and $ErRh_5$.

*Keywords:* R–Rh–B (R=Er; Gd); Rare earth element; $^{166}$Er Mössbauer spectroscopy; $^{155}$Gd Mössbauer spectroscopy; DC magnetization measurement

## 1. Introduction

The $^{166}$Er Mössbauer spectroscopy gives the information on internal magnetic field, magnetic relaxation time and electric quadrupole coupling constant, which can be obtained only in the case of the existence of the internal magnetic field [1–3]. The $^{155}$Gd Mössbauer spectroscopy gives the knowledge about *s* electron density at the nucleus via the isomer shift [2,4–9]. We have made clear that the electrons of the coordinating atoms such as oxygen and nitrogen of the ligands are donated to the 6*s* electron orbital of Gd atom through the coordination bond [8].

The ternary borides of rare earth metal-rich R–Rh–B (R = Er, Gd) system have received considerable attention in the field of superconductivity and magnetism, also in the field of catalysis. But no study has been done from the point of view of chemical bonding. The $^{166}$Er Mössbauer spectroscopic study has not been carried out for the compounds of ER–Rh–B system other than $ErRh_4B_4$, the well-known reentrant magnetic superconductor [1]. In order to elucidate the electronic properties of R–Rh–B (R = Er, Gd) system, we have measured the $^{166}$Er Mössbauer spectra for $ErRh_3B_2$, $ErRh_3B$ and related compounds $ErRh_5$ and $ErRh_2$ and $^{155}$Gd Mössbauer spectra of $GdRh_3B$ and $GdRh_3B_{0.706}$.

## 2. Experimental

### 2.1. Preparation of the compounds

The single crystals of $ErRh_3B_2$ were prepared from the high-purity elements by molten metal flux method using Cu as a flux. The raw materials used were small pieces of 99.9% Er, 99.9% Rh powder and 99.9% B powder. They were weighed at Er:Rh:B = 1:3:2. Cu powder of 99.999% was added to mixture at a weight ratio of 1:10. The mixture was placed in a high-purity alumina crucible. The crucible was inserted in a vertical electric furnace with SiC heater. Throughout the heating, Ar gas was flowed in the furnace for protecting against oxidation. The mixture was heated at a rate of 400 °C h$^{-1}$ and held at 1350 °C for 10 h and then, the solu-

---

☆ Dedicated to Professor Philipp Gütlich’s 70th birthday.

* Corresponding author. Fax: +81 474724175.
*E-mail address:* takda@chem.sci.toho-u.ac.jp (M. Takeda).

0925-8388/$ – see front matter © 2005 Elsevier B.V. All rights reserved.
doi:10.1016/j.jallcom.2005.04.099

tion was slowly cooled down to 1080 °C at a rate of 1 °C $h^{-1}$, followed by cooling to room temperature at 400 °C $h^{-1}$.

### 2.2. *Preparation of $ErRh_3B$, $ErRh_5$, $ErRh_2$, $GdRh_3B$ and $GdRh_3B_{0.706}$*

Polycrystalline samples of these compounds ($ErRh_3B$: [10]) were synthesized by the arc melting method using 99.9% pure Er, Gd, Rh and B as raw materials. The mixture of the starting materials, about 2 g for each sample, was placed in a water-cooled copper hearth in a reaction chamber. Argon was used as a protective atmosphere. The pressure inside the chamber was approximately 1 atm. A small amount of residual oxygen in argon was eliminated by fusing a button of titanium as a reducing agent. The starting materials were then melted for 3 min by an argon arc plasma flame with DC power source at 20 V and 100A. The samples were then turned over and melted three times under the same conditions. Finally, synthesized samples were wrapped in tantalum foil and annealed at 1300 °C for 24 h under vacuum to ensure homogeneity.

### 2.3. *Mössbauer measurement*

The $^{166}Er$ Mössbauer spectra were measured at 12 K by using a $^{166}Ho/Ho_{0.4}Y_{0.6}H_2$ source (1.5 GBq, 41 mCi) prepared with a neutron-irradiation in a JRR-3M reactor. The 55.3 mg of $^{166}Ho_{0.4}Y_{0.6}H_2$ was irradiated for 9 min under the neutron flux of $6.0 \times 10^{13} cm^{-2} s^{-1}$. The absorber thickness was 200 mg Er $cm^{-2}$. A Wissel Mössbauer spectrometer consisting of MDU-1200, DFG-1200 and MVT-1000 was used for acquiring the data [3]. The high-purity germanium solid state detector for low-energy gamma ray measurement was used to detect 80.56 and 86.54 keV Mössbauer gamma rays for $^{166}Er$ and $^{155}Gd$, respectively. The data were analyzed by using the Nowik and Wickman model ($I_g = 0$, $I_e = 2$ for $^{166}Er$ spectra). The $^{155}Gd$ Mössbauer spectra were measured at 12 K by the same way using a $^{155}Eu/^{154}SmPd_3$ source (230 MBq, 6.3 mCi) [4]. The absorber thickness was 150 mg Gd $cm^{-2}$. The data were computer fitted to quadrupole split five lines ($I_g = 3/2$, $I_e = 5/2$, $\eta = 0$) assuming the Lorentzian line shape [11]. For the fitting of the spectra of $ErRh_3B_2$ and $ErRh_5$ (as melted) spin relaxation time was included as a parameter. For the data of $ErRh_3B$ (as melted), $ErRh_3B$ (annealed), $ErRh_2$ (as melted) and $ErRh_2$ (annealed), only one Lorenzian-shaped peak was assumed for fitting.

### 2.4. *Magnetic measurement*

The DC magnetization measurements of $ErRh_2$ (annealed) and $ErRh_5$ (as melted) powder samples were performed using a SQUID magnetometer (MPMS, Quantum Design) between 2 and 300 K in the field strength range of 0.01–5.5 T. For $ErRh_5$ (as melted), magnetic hysteresis loop was also measured at 4.5 K.

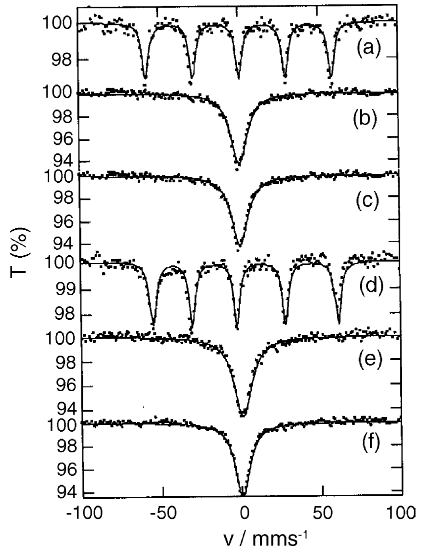

Fig. 1. $^{166}Er$ Mössbauer spectra at 12 K for the erbium compounds of ER–Rh–B system: (a) $ErRh_3B_2$; (b) $ErRh_3B$ (as melted); (c) $ErRh_3B$ (annealed); (d) $ErRh_5$ (as melted); (e) $ErRh_2$ (as melted); (f) $ErRh_2$ (annealed).

## 3. Results and discussion

The $^{166}Er$ and $^{155}Gd$ Mössbauer spectra measured are shown in Figs. 1 and 2, respectively. $ErRh_3B_2$ (Fig. 1a) showed a magnetically splitted five lines Mössbauer spectrum, which agrees well with the fact that this compound is known as a ferromagnet with $T_c = 26.4$ K [12,13]. The effective magnetic field ($H_{eff}$) is determined as 787 ± 1 T. The separations for the five lines are equal and thus the quadrupole coupling constant ($e^2qQ$) is 0 mm $s^{-1}$, showing that the charge distribution around Er nucleus is spherically symmetrical. The crystal structure determination of $ErRh_3B_2$ has revealed that this is a monoclinic system ($C2/m$) where Er atom is surrounded by 20 elements at nearly equal distances whose configuration is $Er Er_2B_6Rh_{12}$ [14].

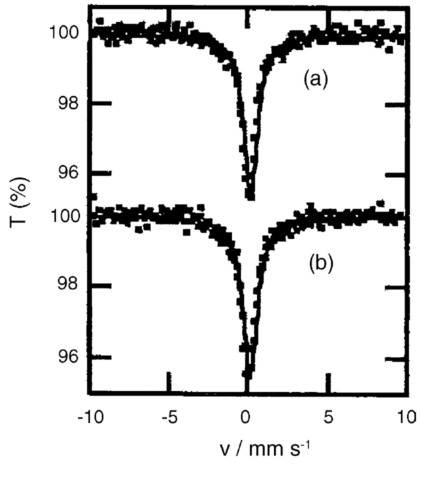

Fig. 2. $^{155}Gd$ Mössbauer spectra at 12 K for $GdRh_3B$ (a) and $GdRh_3B_{0.706}$ (b).

Both $ErRh_3B$ in Fig. 1b and c (as melted and annealed) show single absorption peak without magnetic splitting. This agrees well with its paramagnetism reported [15]. Er atoms occupy A sites of cubic perovskite structure [16], suggesting the high symmetry around the Er atom, whereas the line widths of the sample as melted ($12.8 \pm 0.3\,\mathrm{mm\,s^{-1}}$) and the one annealed ($13.3 \pm 0.3\,\mathrm{mm\,s^{-1}}$) observed are much larger than that ($8.5 \pm 0.2\,\mathrm{mm\,s^{-1}}$) of $ErH_2$ with cubic fluorite structure. This broadening of the line width may be due to the paramagnetic spin relaxation, considering that the quadrupole coupling constant ($e^2qQ$) will be zero for $ErRh_3B$, since $e^2qQ$ is zero for $GdRh_3B$ as described below, which has the same structure as $ErRh_3B$. The Mössbauer spectra of both as melted and annealed samples gave essentially the same ones, suggesting no structural effect of thermal annealing in this case.

The Mössbauer spectrum for $ErRh_5$ (as melted) in Fig. 1d shows existence of both magnetic and quadrupole interactions: $H_{\mathrm{eff}} = 785 \pm 1\,\mathrm{T}$, $e^2qQ = 9.0 \pm 0.2\,\mathrm{mm\,s^{-1}}$, showing the unsymmetrical electron distribution around Er nucleus. $ErRh_5$ has hexagonal $CaCu_5$ type structure and the configuration around Er is $\mathit{Er}Er_2Rh_6Rh_{12}$ [16–18]. Space group is $P6/mmm$; $a$ is 5.118 Å, and $c$ is 4.292 Å [19]. Generally, it is regarded that Rh forms this structure as a high temperature phase from Gd to Lu [17,20]. The observation of large $e^2qQ$ means that the charge distribution around Er nucleus is very much distorted from spherical symmetry. The DC magnetization measurements indeed showed that $ErRh_5$ (as melted) exhibits a smooth ferromagnetic transition ($T_c$) at around 6.0 K. Hysteresis loop measurement at 4.5 K also indicated that this is a soft ferromagnet with very small coercive field (less than 0.01 T), and its saturation moment is $1.145\mu_B$. Since the Mössbauer measuring temperature of 12 K is well above the magnetic transition temperature, the magnetically splitted Mössbauer spectrum observed indicates that the spin relaxation becomes very slow at 12 K; the estimated relaxation time is about 20 ns. The $H_{\mathrm{eff}}$ value is interestingly very close to those of $ErRh_3B_2$ and $ErRh_4B_4$ (767 T) [1] and is larger than that of metallic Er (746 T).

In contrast, $ErRh_2$ in Fig. 1e and f showed again paramagnetic spectra with a broad line width of $14.0 \pm 0.4\,\mathrm{mm\,s^{-1}}$ for the sample as melted and $11.5 \pm 0.2\,\mathrm{mm\,s^{-1}}$ for the annealed sample. This clearly shows that Er sites become more uniform by annealing. The DC magnetization measurements showed that $ErRh_2$ exhibits kink-shaped ferromagnetic transition ($T_c$) at 6.3–6.5 K. $ErRh_2$ is in paramagnetic state in the Mössbauer measurement temperature at 12 K, so the observed large line width will originate from the paramagnetic spin relaxation phenomena. $ErRh_2$ has $MgCu_2$ type structure [21]. Space group is $Fd3m$ (cubic). Lattice constant is 7.444 Å [22]. This structure is categorized as Laves phases [23] *C15* structure type. The lattice is face centered cubic, and the atomic basis consists of two Er atoms and four Rh atoms. Er atoms form a sublattice identical to that of a diamond lattice and the Rh atoms lie at the corners of tetrahedra.

As can be seen in Fig. 2 both $GdRh_3B$ and $GdRh_3B_{0.706}$ show single absorption lines with the fairly small experimental half widths of $1.00\,\mathrm{mm\,s^{-1}}$ showing the high symmetry of surrounding atoms. This agrees well with the symmetrical strucuture around Gd atom. $GdRh_3B$ is of perovskite-type cubic structure: space group $Pm3m$; Z = 1. The lattice parameter $a$ is 4.183(1) Å [24]. The respective isomer shift is $0.11(1)\,\mathrm{mm\,s^{-1}}$ and $0.08(1)\,\mathrm{mm\,s^{-1}}$ and this shows the decrease in the isomer shift as the decrease in the boron content. Since the nuclear parameter $\Delta R/R$ is negative for $^{155}$Gd, the larger the s electron density at the nucleus, the smaller the isomer shift of $^{155}$Gd. Thus the decrease in the boron content makes the *s* electron density at Gd atoms larger, thus we can deduce that the boron atom occupying body center is associated with the chemical bonding.

## 4. Conclusion

$ErRhB_3$ and $ErRh_5$ (as melted) were found to have effective magnetic fields of 787 ± 1 and 785 ± 1 T, respectively. The former is due to ferromagnetic order and the latter is associated with paramagnetic spin relaxation having the relaxation time of ca. 20 ns. In $ErRh_5$, there exists a large electric field gradient at Er nucleus. $ErRh_3B$ (as melted and annealed) and $ErRh_2$ (as melted and annealed) show faster paramagnetic spin relaxation with apparent single Mössbauer absorption peak with large line width. $^{155}$Gd Mössbauer spectra of $GdRh_3B$ and $GdRh_3B_{0.706}$ show the high symmetric environments of surrounding atoms. It was made clear that the boron atom occupying body center is associated with the chemical bonding in Gd–Rh–B system. Magnetic study of $ErRh_2$ (annealed) and $ErRh_5$ (as melted) elucidated that the former does the ferromagnetic transition at 6.3–6.5 K and the latter at 6.0 K.

## Acknowledgements

This research was supported in part by a Grant-in-Aid (No. 10440200) from the Ministry of Education, Culture, Sports, Science and Technology, Japan. This study was performed under the Inter-University Cooperative Research Program of the Laboratory for Advanced Materials, Institute for Materials Research, Tohoku University. The preparation of the Mössbauer source was supported by the Inter-University Joint Research Program using the JAERI facilities. We thank Professor Emeritus of Tohoku University, Tsuguo Fukuda for his encouragement through this work.

## References

[1] G.K. Shenoy, B.D. Dunlap, F.Y. Fradin, S.K. Sinha, C.W. Kimball, W. Potzel, F. Proebst, G.M. Kalvius, Phys. Rev. 21 (1980) 3886.

[2] N.N. Greenwood, T.C. Gibb, Mössbauer Spectroscopy, Chapman and Hall, London, 1971, p. 536.

[3] J. Wang, M. Takahashi, M. Takeda, Bull. Chem. Soc. Jpn. 75 (2002) 735.

[4] J. Wang, J. Abe, T. Kitazawa, M. Takahashi, M. Takeda, Z. Naturforsch. 57a (2002) 581.

[5] J. Wang, M. Takahashi, T. Kitazawa, M. Takeda, J. Radioanal. Nucl. Chem. 255 (2003) 195.

[6] J. Wang, H. Otobe, A. Nakamura, M. Takeda, J. Solid State Chem. 176 (2003) 105.

[7] J. Wang, A. Nakamura, M. Takeda, Solid State Ionics 164 (2003) 185.

[8] M. Takeda, J. Wang, T. Nishimura, K. Suzuki, T. Kitazawa, M. Takahashi, Hyperfine Interact. 156/157 (2004) 359.

[9] A. Nakamura, H. Otobe, J. Wang, M. Takeda, J. Phys. Chem. Solids 66 (2005) 356.

[10] T. Shishido, K. Kudou, S. Okada, J. Ye, M. Oku, H. Horiuchi, T. Fakuda, J. Alloys Compd. 280 (1998) 65.

[11] G.K. Shenoy, B.D. Dunlap, Nucl. Instrum. Meth. 71 (1969) 285.

[12] J. Bernhard, I. Higashi, P. Granberg, L.-E. Tergenius, T. Lundsstrm, T. Shishido, A. Ruokolainen, H. Takei, T. Fukuda, J. Alloys Compd. 193 (1993) 295.

[13] P. Harris, B. Lebech, J. Bernhard, I. Higashi, T. Shishido, H. Takei, T. Fukuda, Jpn. J. Appl. Phys. Ser. 10 (1994) 146.

[14] T. Shishido, J. Ye, M. Oku, S. Okada, K. Kudoh, T. Sasaki, T. Fukuda, T. Matsumoto, J. Alloys Compd. 248 (1997) 18.

[15] H. Takei, N. Kobayashi, H. Yamaguchi, T. Shishido, F. Fukase, J. Less Common Metals 125 (1986) 233.

[16] H. Takei, T. Shishido, J. Less Common Metals 97 (1984) 223.

[17] K. Balkis Ameen, M.L. Bhatia, J. Alloys Compd. 347 (2002) 165.

[18] K.H.J. Buschow, A.S. Van, Dep. Goot. Acta Cryst. B27 (1971) 1085.

[19] A. Raman, H. Ghassem, J. Less Common Metals (1973) 185.

[20] L. Guénée, K. Yvon, J. Alloys Compd. 356/357 (2003) 114.

[21] A.V. Morozkin, Y.D. Seropegin, A.V. Gribanov, J.M. Barakatova, J. Alloys Compd. 256 (1997) 175.

[22] JCPDS, Card No. 17-0001.

[23] G.E.R. Schulze, Z. Elektrochem. 45 (1939) 849.

[24] T. Shishido, J. Ye, S. Okada, K. Kudou, K. Iizumi, M. Oku, Y. Ishizawa, R. Sahara, V. Kumar, A. Yoshikawa, M. Tanaka, H. Horiuchi, A. Nomura, T. Sugawara, K. Obara, T. Amano, S. Kohiki, Y. Kawazoe, K. Nakajima, J. Alloys Compd., in press.